Path planning using sub- and super-harmonic functions ⋆

P. Iñiguez * **J. Rosell** **

* *Dept. Electronics, Electrics and Automatic Engineering*
Rovira i Virgili University, Tarragona, Spain
** *Institute of Industrial and Control Engineering*
Technical University of Catalonia, Barcelona, Spain.

Abstract: One of the main approaches to path planning problems is based on the use of potential fields. Among them, the use of harmonic functions has given interesting results due to its main feature of not having local minima. This paper first analyzes the properties of harmonic functions for path planning and points out the flat region problem as its main disadvantage. Then, to solve this problem, the paper proposes the use of sub- and super-harmonic functions to obtain a better gradient. The method is first developed analytically using the Green function on a 2 d.o.f. configuration space with simple obstacles. Then, a numerical solution using a hierarchical discretization of the configuration space is proposed for its extension to more d.o.f. and obstacles with complex shapes.

1. INTRODUCTION

The path planning problem in robotics consists in the finding of a collision-free path for the robot from an initial to a goal configuration among the obstacles in the workspace. Path planning is usually done in the robot configuration space $\mathcal{C}$, where the robot is reduced to a point and the obstacles are enlarged accordingly. To avoid the explicit construction of the obstacles in $\mathcal{C}$, sampling-based approaches sample configurations of $\mathcal{C}$ and capture the connectivity of the free regions by connecting those that are collision-free (when possible) forming either roadmaps [Kavraki and Latombe, 1994] or trees [Kuffner and LaValle, 2000].

Other approaches, sometimes called feedback motion planning strategies [LaValle, 2006], focus on the situations where the existence of a nominal solution path is not enough to guarantee the successful performance of a task, even if feedback control laws are used to follow it. Feedback motion planning strategies assume that any unexpected configuration can be achieved (i.e. implicitly consider uncertainty) and therefore provide a feedback plan with the proper action to be applied from any configuration to allow the robot reaching the goal. These strategies are used for example in mobile robotics [Prestes et al., 2002] or haptic guidance [Rosell et al., 2008]. Feedback plans are usually defined using the gradient descent of potential functions [Khatib, 1986], called navigation functions when they have a single minimum at the goal configuration [Latombe, 1991, Yang and LaValle, 2004].

The combination of sampling-based methods with potential fields has been proposed either by using potential fields to bias the samples towards difficult regions of $\mathcal{C}$ [Aarno et al., 2004], or by using sampling methods to explore $\mathcal{C}$ to obtain a cell decomposition model where to compute a potential field [Lingelbach, 2004, Rosell and Iñiguez, 2005].

Among the potential field approaches, those based on harmonic functions are interesting because they give rise to practical, resolution-complete planners without local minima [Souccar et al., 1998]. An harmonic function ϕ on a domain $\Omega \subset \mathbb{R}^n$ is a function that satisfies Laplace's equation:

$$div\,(grad\ u) = 0 \quad \Rightarrow \quad \nabla^2 u = 0 \tag{1}$$

The solution of Laplace's equation can be analytically found for easy problems [Farlow, 1993]. For more complex situations it is usually numerically computed. The properties of harmonic functions from the path planning perspective are the following:

1) *Nonexistence of local minima:* The main advantage of harmonic functions for path planning is the nonexistence of local minima in the domain. This determines that a path planner based on harmonic function be complete, i.e. it will found a solution if it exists. This property arises applying the locality principle [DuChateau and Zachmann, 1986]. Considering for simplicity the case of a function in two dimensions, of C^2 class, and a circumference B_R of radius R and contour L with center at point $\boldsymbol{r}_0 = (x_0, y_0)$. By the locality principle, the value of u at this point is:

$$u_0 = u(x_0, y_0) = \frac{1}{2\pi R}\oint_L u(x,y)dl - \frac{R}{4} div\,(\text{grad } u)_{\boldsymbol{r}_0}\,, \tag{2}$$

where the first term is the mean value of the function in B_R and the second depends on the Laplacian of the function at the central point and determines the change in the gradient at that point with respect to the local domain B_R. If the Laplace equation is satisfied then:

⋆ This work was partially supported by the CICYT projects DPI2007-63665 and DPI2008-02448.

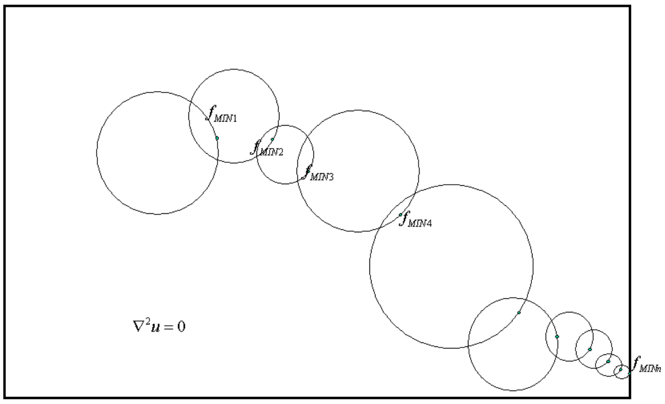

Fig. 1. The minimum of a harmonic function is found in the contour.

$$u(x_0, y_0) = \frac{1}{2\pi R} \oint_L u(x,y) dl, \tag{3}$$

which determines that $u(x_0, y_0)$ cannot be an extreme value of u within B_R. Since this is satisfied in all the points of the whole domain, the minimum and maximum values are always found in the boundary, as illustrated in Fig. 1.

2) *Regularity of the solution:* The curvature of the solution streamlines obtained following the gradient of a harmonic function is optimally smooth. This is an advantage when robot dynamics must be taken into account to follow the trajectory.

3) *Stability of the solution:* Small changes in the boundary conditions imply small changes in the solution. This is important (and essential in dynamic scenarios) since the computational cost of updating the solution when changes occur will be minimum.

4) *Gradient of the solution:* The main disadvantage of using harmonic functions for path planning is the non-uniform distribution of the gradient and the difficulty it entails its following in those regions where it has very small values (flat regions, Fig. 2). Consider a non-boundary problem with a delta function located at the goal configuration $\boldsymbol{r}_d$. Then, $\nabla^2 u = \delta(\boldsymbol{r}_d)$, and applying the divergence theorem in a hypersphere centered at $\boldsymbol{r}_d$ results:

$$\oint_S \nabla u \cdot d\boldsymbol{S} = \int_V (\nabla \cdot \nabla u)\, dV = \int_V \delta(\boldsymbol{r}_d)\, dV = 1 \tag{4}$$

This means that the flux of the gradient through any surface enclosing the delta function is constant and equal to 1 (Gauss theorem), and therefore the farther the surface from $\boldsymbol{r}_d$, the smaller the gradient over its points. Considering the surface of a hypersphere and using the symmetry of the model:

$$\nabla u = \frac{1}{S_n} \frac{\boldsymbol{r} - \boldsymbol{r}_d}{\|\boldsymbol{r} - \boldsymbol{r}_d\|}, \tag{5}$$

where S_n is the surface of a hypersphere of radius R, i.e. $S_n = n k_n R^{n-1}$, with n the dimension of the space and $k_n = \pi,\ \frac{4}{3}\pi,\ \frac{1}{2}\pi^2, \ldots$ for $n = 2,\ 3,\ 4,\ 5, \ldots$. If the radius of the hypersphere is big and the dimension of the space too, then the modulus of the gradient can be very small, even below the computer precision, making the approach useless.

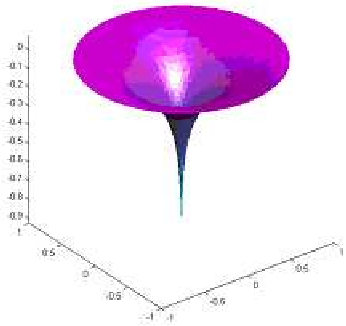

Fig. 2. The landscape of the harmonic function shows the flat region problem encountered far form the goal configuration $\boldsymbol{r}_d$ where a delta function is located.

2. PROPOSED APPROACH: ANALYTICAL SOLUTION

In order to solve the flat region problem, this paper proposes the use of sub-harmonic and super-harmonic functions. Sub-harmonic functions are those functions that satisfy $\nabla^2 u \geq 0$ on a given domain Ω and the super-harmonic functions are those that satisfy $\nabla^2 u \leq 0$ [DuChateau and Zachmann, 1986].

Considering for simplicity the case of a sub-harmonic function in two dimensions u, with regularity C^2, that satisfies $\nabla^2 u = \rho$ with $\rho \geq 0$, and a circumference B_R of radius R and contour L with center at point $\boldsymbol{r}_0 = (x_0, y_0)$. From (2):

$$u_0 = u(x_0, y_0) = \frac{1}{2\pi R} \oint_L u(x,y) dl - \frac{R}{4}\rho(x_0, y_0) \tag{6}$$

Therefore, being $u_{\mathrm{MIN}(L)}$ and $u_{\mathrm{MAX}(L)}$ the minimum and maximum values of u at L:

$$u_{\mathrm{MIN}(L)} - \frac{R}{4}\rho(\boldsymbol{r}_0) < u_0 < u_{\mathrm{MAX}(L)} - \frac{R}{4}\rho(\boldsymbol{r}_0), \forall \boldsymbol{r}_0 \in \Omega, \tag{7}$$

which implies that the maximum of the function (over the region B_R) is found over its boundary while the minimum is found over its boundary or in the interior (Fig. 3).

In a similar way for a super-harmonic function satisfying $\nabla^2 u = -\rho$ with $\rho \geq 0$:

$$u_{\mathrm{MIN}(L)} + \frac{R}{4}\rho(\boldsymbol{r}_0) < u_0 < u_{\mathrm{MAX}(L)} + \frac{R}{4}\rho(\boldsymbol{r}_0), \forall \boldsymbol{r}_0 \in \Omega, \tag{8}$$

which implies that the minimum of the function (over the region B_R) is found over its boundary while the maximum is found over its boundary or in the interior (Fig. 3).

Having in mind these properties, this paper proposes to maintain a delta function at the goal configuration $\boldsymbol{r}_d$, as usually done, and:

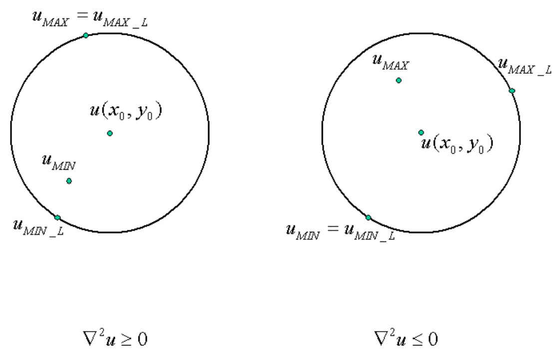

Fig. 3. Extremes of sub- and super-harmonic functions over a local domain.

a) To model the surroundings of the goal configuration as a region $\Omega_P \subset \Omega$ where u is sub-harmonic. Although a sub-harmonic function can have local minima within the region where it is defined, this won't be the case since Ω_P surrounds the goal configuration where the delta function forces the global minimum. And, as a benefit, the existence of Ω_P will shape u with a deep valley around the goal configuration, increasing the gradient of u in regions where, otherwise, it would be too small for navigation purposes due to the flat region problem.

b) To model the obstacles as a region $\Omega_O \subset \Omega$ where the function u is super-harmonic. Treating the obstacles as super-harmonic regions instead of borders (with a boundary condition) of the domain where a harmonic function is computed, as usually done, makes the method more flexible for its combination with sampling methods that explore the configuration space [Rosell et al., 2008].

Then, the navigation function u at any point $p \in \Omega$ satisfies:

$$\nabla^2 u = \rho + \delta(\boldsymbol{r}_d), \tag{9}$$

where:

$$\rho = \begin{cases} -\rho_O \ \forall p \in \Omega_O \\ \rho_P \ \forall p \in \Omega_P \\ 0 \ \forall p \notin (\Omega_O \cup \Omega_P) \end{cases} \tag{10}$$

being $\rho_O \geq 0$ and $\rho_P \geq 0$ constant values.

Now, applying the divergence theorem the following is obtained:

$$\oint_S \nabla u \cdot d\mathbf{S} = \int_V \nabla^2 u dV = 1 + (\rho_P V_P - \rho_O V_O), \tag{11}$$

where V_O and V_P are, respectively, the volumes of the obstacles (region Ω_O) and of the region Ω_P. Choosing adequately the values of ρ_O and ρ_P, the flux of the gradient can be properly balanced between the obstacle "mountains" and the goal "valley", obtaining a more regular distribution all over the space.

Subsection 2.1 presents the procedure to analytical obtain the solution of the navigation function u using the Green function, and subsection 2.2 illustrates it with a simple example.

2.1 Analysis using the Green function

The use of the first and second Green theorems allows isolating the influence of the boundary conditions over the potential function and its properties [Haberman, 1998]. The Green function on a domain Ω is defined as the solution of the following equation:

$$\nabla^2 G = \delta(\boldsymbol{r}), \tag{12}$$

being $\boldsymbol{r}$ any point in Ω and considering homogeneous boundary conditions. Then, for the model $\nabla^2 u = \rho + \delta(\boldsymbol{r}_d)$ with non-null boundary conditions, the second Green theorem gives:

$$u(\boldsymbol{r}) = g(\boldsymbol{r}, \boldsymbol{r}_d) + \int_V \rho G dV_0 + \oint_S \left(u \frac{\partial G}{\partial \mathbf{n}} - G \frac{\partial u}{\partial \mathbf{n}} \right) dS_0, \tag{13}$$

where:

- $g(\boldsymbol{r}, \boldsymbol{r}_d)$ is the response to the delta function.
- The volume integral determines the influence of the sub- and super-harmonic regions
- The surface integral represents the boundary conditions of the workspace:

  Dirichlet boundary condition: $-\oint_S \left(u \frac{\partial G}{\partial \mathbf{n}} \right) dS_0$

  Neumann boundary condition: $\oint_S \left(G \frac{\partial u}{\partial \mathbf{n}} \right) dS_0$

2.2 An example

Equation (13) has been programmed in Matlab for the case of two-dimensional spaces with circular obstacles, modelling region Ω_O as a set of circular rings, one for each obstacle, with $\rho = -\rho_O$, and region Ω_P as a single ring with $\rho = \rho_P$.

Figure 4a shows a particular example with two obstacles (light blue rings) where the function is super-harmonic and a goal configuration encircled by a circular ring (dark blue) where the function is sub-harmonic.

The contribution to the solution of the different terms of (13) is the following:

a) The contribution of the delta function located at the goal configuration, shown in Fig. 4b.

b) The contribution of the circular rings where the function is either sub- or super-harmonic, shown in Fig. 4c.

c) The contribution of the boundary conditions is null, since no boundary has been considered in this example.

The global effect is shown in Fig. 4d, where it can be seen that the consideration of sub- and super-harmonic functions gives a better gradient, avoiding the flat region problem that appear if only harmonic functions are considered.

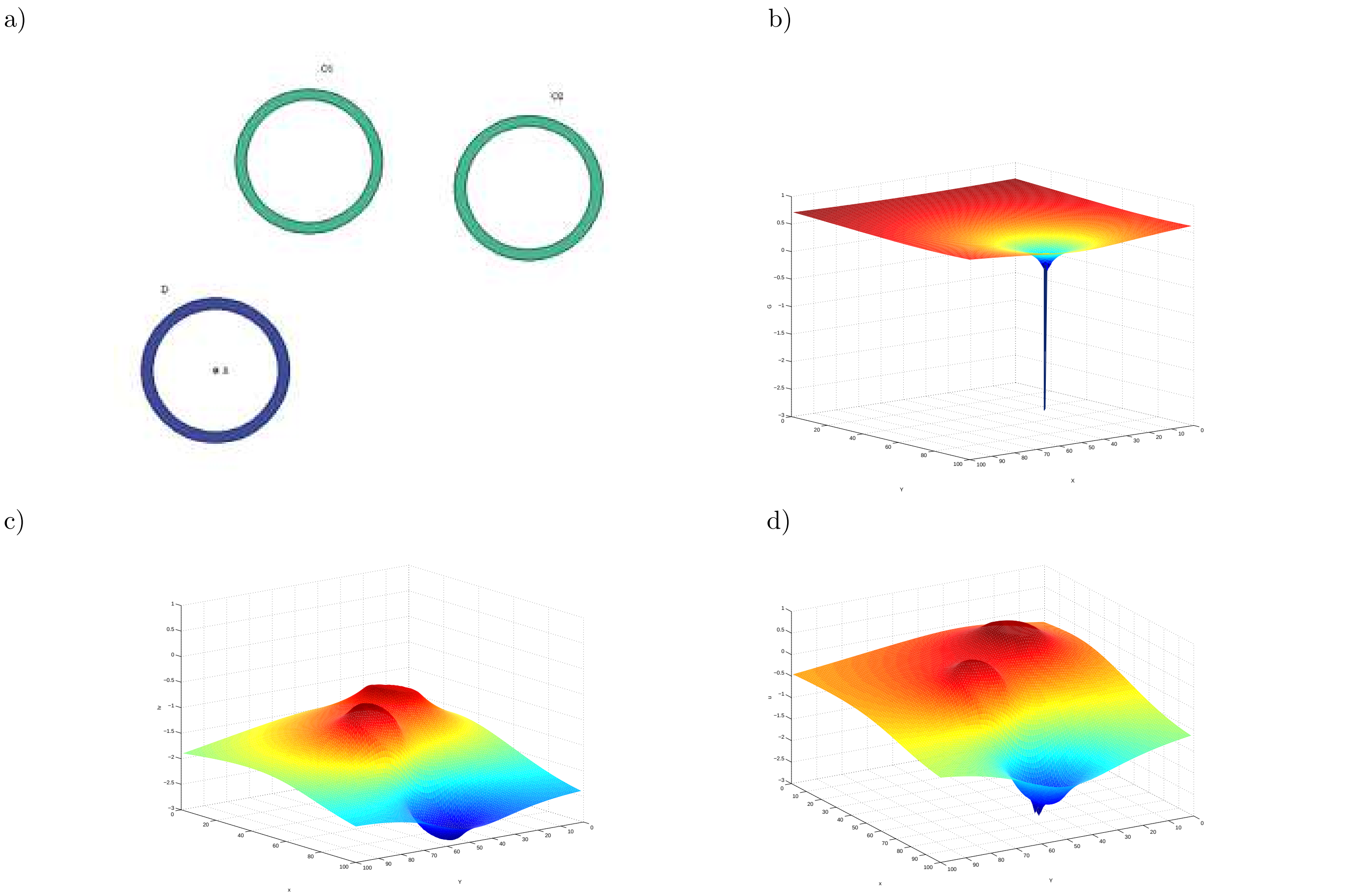

Fig. 4. a) Regions Ω_O (light blue) and Ω_P (dark blue); b) Response to the delta function located at the goal configuration; c) Response due to the sub- and super-harmonic regions; d) Resulting navigation function.

3. PROPOSED APPROACH: NUMERICAL SOLUTION

3.1 Solution over a regular cell decomposition

In order to obtain a numerical solution of a differential equation the equivalent difference equation over a discretized space has to be solved using iterative methods.

Consider a uniform grid over a two-dimensional space. Given u_0, the value of u at the cell with center at $\boldsymbol{r}_0 = (x_0, y_0)$, the value of u at its neighbor cells can be computed by Taylor as (Fig. 5):

$$\begin{aligned}
u(x_0+h, y_0) &= u(x_0, y_0) + \frac{1}{1!}\frac{\partial u}{\partial x}\Big|_{(x_0,y_0)} h + \frac{1}{2!}\frac{\partial^2 u}{\partial x^2}\Big|_{(x_0,y_0)} h^2 + \ldots \\
u(x_0-h, y_0) &= u(x_0, y_0) - \frac{1}{1!}\frac{\partial u}{\partial x}\Big|_{(x_0,y_0)} h + \frac{1}{2!}\frac{\partial^2 u}{\partial x^2}\Big|_{(x_0,y_0)} h^2 - \ldots \\
u(x_0, y_0+h) &= u(x_0, y_0) + \frac{1}{1!}\frac{\partial u}{\partial y}\Big|_{(x_0,y_0)} h + \frac{1}{2!}\frac{\partial^2 u}{\partial y^2}\Big|_{(x_0,y_0)} h^2 + \ldots \\
u(x_0, y_0-h) &= u(x_0, y_0) - \frac{1}{1!}\frac{\partial u}{\partial y}\Big|_{(x_0,y_0)} h + \frac{1}{2!}\frac{\partial^2 u}{\partial y^2}\Big|_{(x_0,y_0)} h^2 - \ldots
\end{aligned} \tag{14}$$

Adding them gives:

$$\sum_{i=1}^{4} u_i = 4u_0 + \sum_{k=1}^{\infty} \frac{2h^{2k}}{2!} \nabla^{2k} u_0 \tag{15}$$

The extension to n dimensions is:

$$\sum_{i=1}^{2n} u_i = 2nu_0 + \sum_{k=1}^{\infty} \frac{nh^{2k}}{2!} \nabla^{2k} u_0 \tag{16}$$

From this, the value of u_0 can be expressed as:

$$u_0 = \frac{1}{2n} \sum_{i=1}^{2n} u_i - \sum_{k=1}^{\infty} \frac{h^{2k}}{2 \cdot 2!} \nabla^{2k} u_0 \tag{17}$$

For harmonic functions it is satisfied that $\nabla^2 u = 0$ and $\nabla^{2k} u = 0$ with $k = 1, 2, 3, \ldots$. Therefore:

$$u_0 = \frac{1}{2n} \sum_{i=1}^{2n} u_i, \tag{18}$$

which represents the mean value of the Manhattan neighbors of the cell.

For sub- and super-harmonic functions, taking into account that $\nabla^2 u = \rho$ and $\nabla u \cdot \mathbf{n} = \frac{\partial u}{\partial \mathbf{n}}$ the following is obtained:

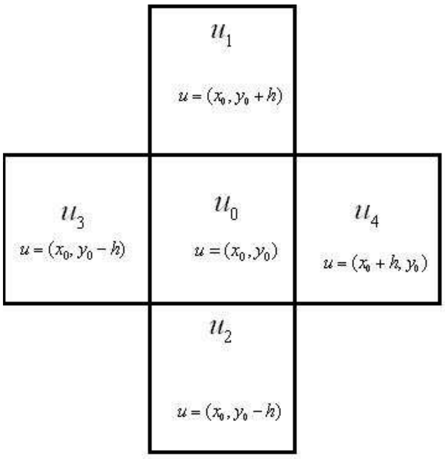

Fig. 5. Regular grid for the computation of u.

$$\nabla^{2k} u = \frac{\partial^{2(k-1)}\rho}{\partial \mathbf{n}^{2(k-1)}} \quad k = 1, 2, 3, \ldots \tag{19}$$

And the value of u_0 results:

$$u_0 = \frac{1}{2n}\sum_{i=1}^{2n} u_i - \frac{1}{2 \cdot 2!}\sum_{k=1}^{\infty} h^{2k} \left.\frac{\partial^{2(k-1)}\rho}{\partial \mathbf{n}^{2(k-1)}}\right|_{\mathbf{r}_0} \tag{20}$$

Considering constant values of ρ, this expression can be simplified to:

$$u_0 = \frac{1}{2n}\sum_{i=1}^{2n} u_i - H\rho(\boldsymbol{r}_0), \tag{21}$$

with $H = \frac{h^2}{2 \cdot 2!}$ and the expression of ρ given by (10).

The Jacobi relaxation method obtains u all over the grid, by iteratively applying (21), i.e. being m the iteration step, $\boldsymbol{r}$ the center of a general cell of the grid, and arbitrarily setting $H = 1$:

$$u_{\boldsymbol{r}}^{m+1} = \frac{1}{2n}\sum_{i=1}^{2n} u_i^m - \rho(\boldsymbol{r}) \tag{22}$$

Other relaxation methods can be also used, like the Gauss-Seidel or S.O.R..

3.2 Solution over a hierarchical cell decomposition

For path planning purposes the objective is to compute a navigation function whose gradient descent leads to the goal. This navigation function needs not be computed over a fine regular grid, but for computational efficiency purposes it can be computed over a hierarchical cell decomposition (a 2^n-tree) with big cells over uniform regions of the configuration space.

The use of harmonic functions over a hierarchical cell decomposition has been previously proposed by the authors [Iñiguez and Rosell, 2003]. In the present approach the method is extended to the computation of sub- and super-harmonic functions.

Consider a 2^n-tree decomposition of the configuration space. The initial cell with sides with unitary size is

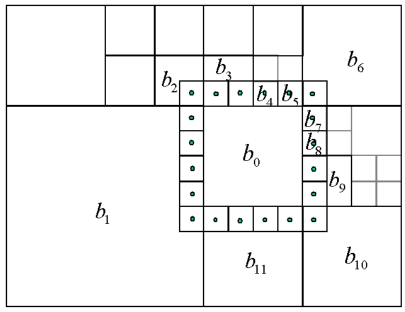

Fig. 6. Computation of u over a hierarchical cell decomposition of the configuration space.

the tree root. The levels in the tree are called partition levels (a cell of a given partition level m is called an m-cell). Partition levels are enumerated such that the tree root is the partition level 0 and the maximum resolution corresponds to partition level M. Then, the value of u at a given m-cell b_0 is computed by modifying the first term of (21). This term changes from a mean of the values of u at the neighbor cells, to a weighted mean, i.e.:

$$u_0 = \frac{1}{N_{max}}\sum_{i=1}^{N} W_i u_i - \rho(\boldsymbol{r}_0), \tag{23}$$

where:

- N is the actual number of neighbor cells.
- N_{max} is the maximum number of neighbor M-cells that an m-cell can have:
$$N_{max} = 2n2^{(n-1)(M-m)}, \tag{24}$$
n being the dimension of the space.
- W_i is the size of the border between two neighbor cells measured in M-cells. If the partition level of the ith neighbor is p_i, then:
$$W_i = 2^{(n-1)(M-\max(m-p_i))} \tag{25}$$
- ρ has the expression given in (10).

As an example, consider a two-dimensional configuration space decomposed as a quadtree, like the one shown in Fig. 6. Using (23), the value of u at cell b_0 centered at $\boldsymbol{r}_0$ is:

$$u_0 = \frac{4u_1 + 2u_3 + u_4 + u_5 + u_7 + u_8 + 2u_9 + 4u_{11}}{16} - \rho(\boldsymbol{r}_0) \tag{26}$$

Finally, the relaxation of u is obtained, using the Jacobi method, by the following expression:

$$u_{\boldsymbol{r}}^{m+1} = \frac{1}{N_{max}}\sum_{i=1}^{N} W_i u_i^m - \rho(\boldsymbol{r}) \tag{27}$$

3.3 A numerical example

Fig. 7 shows an example equivalent to the one shown in Section 2.2. In this example the obstacles have a free a)

b)

c)

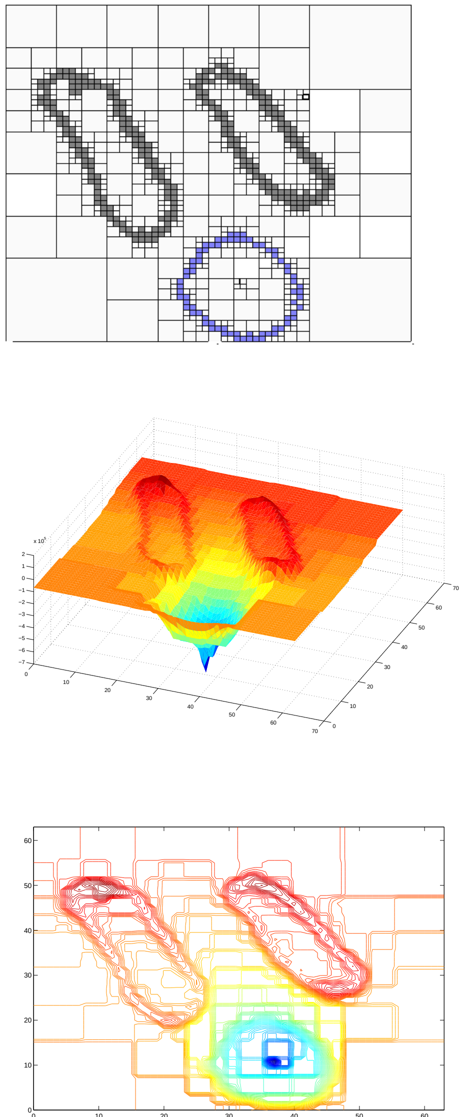

Fig. 7. a) Hierarchical partition of the configuration space with regions Ω_O and Ω_P; b) Resulting numerical navigation function; c) corresponding equipotential lines.

form and wide open regions are modelled by big cells of the hierarchical cell decomposition. The landscape of the navigation function obtained demonstrates that the use of sub- and super-harmonic functions gives a good gradient, overcoming the flat region problem encountered when only harmonic functions are used.

4. CONCLUSIONS AND DISCUSSION

Harmonic functions where initially proposed as a good alternative to implement the potential field path planning approach due to the absence of local minima. Nevertheless, they have a drawback, namely the flat region problem that makes that far away from the goal configuration the gradient may be too small. The problem worsens for increasing degrees of freedom and when using numerical solution by means of relaxation methods. This may carry practical problems that may advise against the use of such a method. To recover from this problem, the paper presented the used of sub- and super-harmonic functions that allow to properly shape the navigation function. The approach has been demonstrated analytically using the Green function for simple scenarios (two-dimensional configuration space with circular obstacles), and also using a numerical solution computed over a hierarchical discretization of the configuration space for its extension to more complex scenarios.

REFERENCES

D. Aarno, D. Kragic, and H. I. Christensen. Artificial potential biased probabilistic roadmap method. In *Proc. of the IEEE Int. Conf. on Robotics and Automation*, pages 461–466, 2004.

P. DuChateau and D. W. Zachmann. *Partial differential equations*. Schaum's Outlines, 1986.

S. F. Farlow. *Partial differential equations for Scientists and Engineers*. Dover Books on Mathematics, 1993.

R. Haberman. *Elementary Applied Partial Differential Equations*. Prentice Hall, 1998.

P. Iñiguez and J. Rosell. Probabilistic harmonic-function-based method for robot motion planning. In *Proc. of the IEEE/RSJ Int. Conf. on Intelligent Robots and Systems*, pages 382–387, 2003.

L. E. Kavraki and J.-C. Latombe. Randomized preprocessing of configuration for fast path planning. In *Proc. of the IEEE Int. Conf. on Robotics and Automation*, volume 3, pages 2138–2145, 1994.

O. Khatib. Real-time obstacle aboidance for manipulators and mobile robots. *Int. Journal of Robotics Research*, 5 (1):90 – 98, 1986.

J. J. Kuffner and S. M. LaValle. RRT-connect: An efficient approach to single-query path planning. In *Proc. of the IEEE Int. Conf. on Robotics and Automation*, pages 995–1001, 2000.

J.-C. Latombe. *Robot Motion Planning*, chapter Potential Field Methods, pages 296 – 355. Kluwer Academic Publishers, 1991.

S. M. LaValle. *Planning Algorithms*, chapter Feedback Motion Planning, pages 367 – 430. Cambridge University Press, 2006.

F. Lingelbach. Path planning using probabilistic cell decomposition. In *Proc. of the IEEE Int. Conf. on Robotics and Automation*, pages 467–472, 2004.

E. Prestes, P. M. Engel, M. Trevisan, and M. A. P. Idiart. Exploration method using harmonic functions. *Robotics and Autonomous Systems*, 40:25–42, 2002.

J. Rosell and P. Iñiguez. Path planning using harmonic functions and probabilistic cell decomposition. In *Proc. of the IEEE Int. Conf. on Robotics and Automation*, pages 1815–1820, 2005.

J. Rosell, C. Vázquez, A. Pérez, and P. Iñiguez. Motion planning for haptic guidance. *J. of Intelligent and Robotic Systems*, 53(3):223–245, 2008.

K. Souccar, J. Coelho, C. Connolly, and R. Grupen. *Practical Motion Planning in Robotics*, chapter Harmonic Functions for Path Planning and Control, pages 277–301. John Wiley & Sons Ltd, 1998.

L. Yang and S. M. LaValle. The sampling-based neighborhood graph: An approach to computing and executing feedback motion strategies. *IEEE Trans. on Robotics and Automation*, 20(3):419– 432, 2004.